

Influence of Hexagonal Textures on the Performance of Hydrodynamic Journal Bearing

Aman Gupta^{1*}, Mohammad Arif², Nitin Sharma³ and Saurabh Kango⁴

¹M.Tech Student, Department of Mechanical Engineering, Dr. B. R. Ambedkar National Institute of Technology
Jalandhar 144027, Punjab, India

²Ph.D Scholar, Department of Mechanical Engineering, Dr. B. R. Ambedkar National Institute of Technology,
Jalandhar 144027, Punjab, India

^{3,4}Assistant Professor, Department of Mechanical Engineering, Dr. B. R. Ambedkar National Institute of Technology,
Jalandhar 144027, Punjab, India

E-mail: ¹amang.de.21@nitj.ac.in, ²ma40360@gmail.com, ³sharman@nitj.ac.in, ⁴kangos@nitj.ac.in

Abstract—The present study reveals the feature of hexagonal textures by evaluating the tribological performance of journal bearing. The Reynolds equation has been utilized as governing equation and the film thickness equation has been modified to include the effects of textures. The bearing performance characteristics such as fluid film pressures, film thickness, etc. have been calculated by taking different zones of textures and are compared with the plain journal bearing case. A MATLAB code has been developed for the numerical calculations related to tribological properties. The results witnessed that the inclusion of textures in the right location will enhance the journal-bearing performance. Moreover, the results are well validated with the previous work and computed by varying the eccentricity ratio, shaft speed, dimple depth, etc.

Keywords: hexagonal texture, hydrodynamic lubrication, journal bearing, fluid film pressure

1. INTRODUCTION

Many researchers have developed a variety of methods over the last two decades to improve the hydrodynamic bearing performance such as enhancing the lubrication features and providing textures on the bearing surface at different locations via different techniques. The bearing characteristics of the sliding bearing are greatly affected by the shapes and geometry of the surface textures. For each texture shape geometry and density are optimized with respect to friction coefficient. In most studies, the authors investigated the performance of journal bearing and found that the different shape textures/dimples have attained the best tribological characteristics [1]–[5].

The surface texture is used to reduce friction in real-life applications such as piston rings in the automotive industry. Additionally, it can be used to enhance the functionality of journal bearings. There are various other uses of textures, for example, they served as micro lubricant reservoirs and also

collect dirt and sharp particles which avoids surface damage [6]. the texture's depth and area are some essential geometric parameters which play a crucial role in improving/depriving the bearing performance. Various sizes and different types of dimples have been created on either moving surfaces or stationary surfaces. Textures have been shown to have a positive impact on load capacity and friction reduction [7].

The tribological applications, which typically range from equipment for manufacturing use to large applications such as turbines, have lately revived curiosity in and value for this field. Hydrodynamic bearings have been used for a very long time in a variety of designs and applications [8]. The development of inducing texture in bearing design is gaining popularity and is anticipated to play a significant role in the design of future bearings. The goal of the current work is to develop journal-bearing surfaces with a deterministic hexagonal texture and evaluate their tribological performance characteristics at different locations (zones) that provide lubrication within the hydrodynamic location.

2. MATHEMATICAL & NUMERICAL FORMULATION

In Figure 1. A schematic representation of hydrodynamic journal bearing is shown. Where the bearing geometry has been presented with shaft radius R , bearing length L , and journal angular velocity ω . The variation in film thickness produced by the surface's texture, (ϵ) is the journal's eccentricity, and Cr is a radial clearance of the bearing. The rupture zone of the film is identified using the boundary conditions, also referred to as Reynolds boundary conditions. The applied load F is a constant and its direction is vertical in the case of the current study, where the bearing works under steady-state conditions. Through the numerical integration

of the pressure field along the journal bearing's surface contact area, the total load (L_r) is determined [8].

The Reynolds equation has been used to determine the parameters affecting bearing performance. The fluid film pressure in the journal bearing is then determined by discretizing this equation via the finite difference method. The tribological property such as load-carrying capacity is calculated using Simpson's 1/3 rule. The flow is considered as a laminar and the inertia is neglected. The fluid is incompressible and Newtonian. It is also supposed that the density and viscosity are both constant. The following equation determines the pressure on the lubricating film to the journal running at a steady state [9].

$$\frac{\partial}{\partial x} h^3 \frac{\partial p}{\partial x} + \frac{\partial}{\partial z} h^3 \frac{\partial p}{\partial z} = 6\eta U \frac{\partial h}{\partial x} \quad (1)$$

The *MATLAB* code has been developed from the discretization of the equation. The following convergence criteria has been considered for the computation of the results

$$\sum \sum \left| \frac{(P_{i,j})_k - (P_{i,j})_{k-1}}{(P_{i,j})_k} \right| < 10^{-8} \quad (2)$$

Where,

$i \rightarrow$ Total number of nodes in circumferential directions

$j \rightarrow$ Total number of nodes in the axial directions

$k \rightarrow$ Number of iterations

P stands for lubricant pressure, h for film thickness, and η for dynamic viscosity in equation (1). And a non-linear oil film thickness has been formed by journal bearing forming convergent-divergent zones given by

$$h = Cr(1 + \epsilon \cos\theta) \text{ without texture} \quad (3)$$

$$h = Cr(1 + \epsilon \cos\theta) + h_t \text{ with texture} \quad (4)$$

The convergence & grid independent tests are taken into consideration for validating the present numerical model. At a pressure convergence of 10^{-8} , the pressure values are in accordance. Based on the grid independence test, 223 nodes along the circumferential direction, as well as 72 nodes in the axial direction.

2.1 Pressure boundary conditions

The analysis utilizes the Reynolds pressure boundary conditions. The bearing edges are under no pressure at all. During computation, the magnitude of positive pressures is determined, and the negative pressures are set to zero.

2.2 Load-carrying capacity

The load-carrying capacity of the journal bearing is calculated as:

$$L_r = \sqrt{(load_x)^2 + (load_y)^2} \quad (5)$$

$$load_x = \int_0^1 \int_0^{2\pi r} P \cos\theta d\theta$$

$$load_y = \int_0^1 \int_0^{2\pi r} P \sin\theta d\theta$$

3. SURFACE TEXTURES

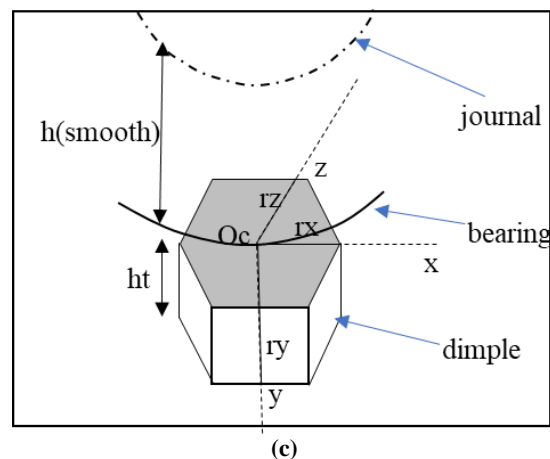
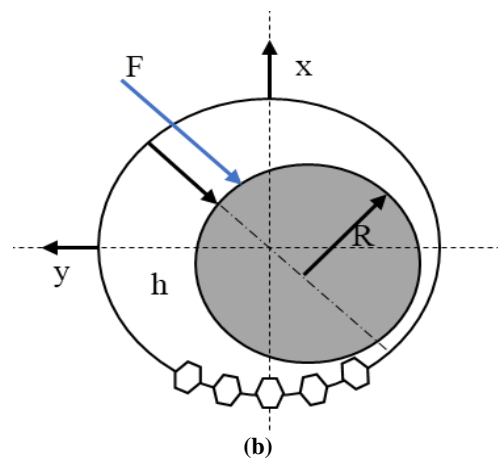
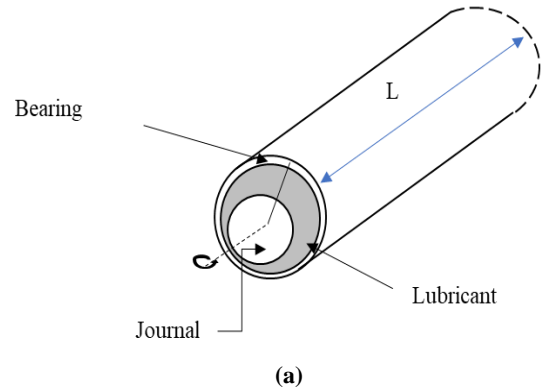


Figure 1: Schematic representation of hydrodynamic journal bearing (a) Pictorial representation of Journal and bearing; (b) representation of textures on the surface of bearing; (c) Details of texture geometry.

In the present work, the bearing surface has been added with hexagonal surface textures as witnessed by previous investigators [9],[10]. Partial textures have been offered in the circumferential direction along with the axial direction (0° to 180°). Figure 1(c). shows the hexagonal texture shapes that were used in this study. where the textured center's three coordinates are (x, y, and z). According to Figure 1. The Center Oc along with (rx, ry, and rz) represent the texture's dimensions for the x, y, and z directions, respectively and the depth of texture is defined by (ht=0.3*Cr).

4. INFLUENCE OF TEXTURE DIMENSIONS

Table 1. shows the validation of the present model by the results of load carrying capacity has been given by referencing the work of Kango et al [10]. The values of the critical parameters in a lubricated journal bearing are computed.

The hexagonal texture is used to analyze the texture size affecting lubrication properties. The parameters $N_{tx}=8$ and $N_{tz}=4$ define the number of textures in the circumferential and axial directions, respectively. Just an appropriate distribution of textures on the bearing surface can positively impact the key elements of a lubricated contact and enhance the performance of the journal-bearing system. Figure 2. Shows the unfolded view of the journal-bearing surface including the distribution of textures in the axial and circumferential direction. Where figure (a) represents partial textures (from 0° to 180°). And (b) full textures (from 0° to 360°).

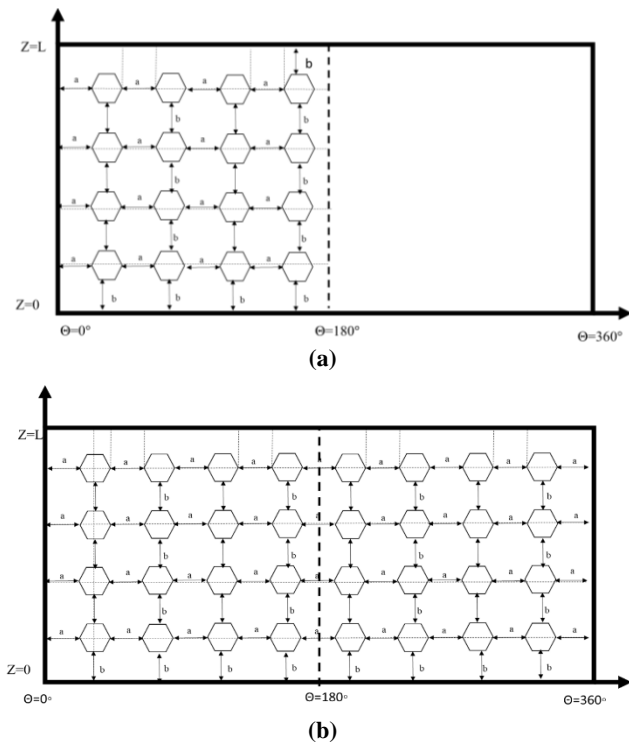


Figure 2: Unfolded view of journal-bearing surface including distribution of textures in the axial and circumferential direction. (a) partially textured (from 0° to 180°). (b) fully textured (from 0° to 360°).

5. RESULTS AND DISCUSSION

Table 2. has been provided for the input data. The results reveal the numerical calculations of various tribological properties for journal bearing such as fluid film thickness, fluid film pressure, etc. The results computed from the present model are in good correlation with the previous work.

Table 1: Validation of the present model via results of load carrying capacity with the work of Kango et al [10].

Parameters		Kango et al. [10]	Present work
N (RPM)	Eccentricity (ε)	Lr (resultant load) in N	Lr (resultant load) in N
1500	0.3	1316	1313.6
	0.7	6577	6562.3
3000	0.3	2632	2627.2
	0.7	13150	13125

In this work, the hexagonal texture has been incorporated to test the properties of journal bearing. Two texture zone has been selected; zone 1 and zone 2. The eccentricity ratio is 0.3 & 0.7 and the shaft speed is 1500 & 3000 rpm. Total textures on the bearing surface are taken according to the geometric arrangement of textures on the bearing surface, 16 and 32 textures are considered in partial and full texture zone respectively. Table 3. Shows the results for minimum film thickness and maximum fluid film pressure for both considered zones.

Table 2: Input data

Input parameters	values
Eccentricity ratio (ε)	0.3-0.7
Shaft speed (N), rpm	1500,3000
Radial Clearance (Cr), m	50 x 10 ⁻⁶
Shaft Radius (R), m	0.02
Bearing length (L), m	0.04
Length of bearing in Z-direction	2*R
Viscosity (Pa-s)	0.08
Angular velocity (ω)	2*pi*N/60
Journal velocity(U)	(ω)*(R)
Nodes in the axial direction (Nx)	223
Nodes in the circumferential direction (Nz)	72
Number of textures in the circumferential direction	8
Number of textures in the axial direction	4

Length of hexagonal texture	0.006
Width of hexagonal texture	0.0057
Depth of hexagonal texture	0.3*Cr

Table 3: Tribological characteristics of the partial and full texture zones (zone 1 and zone 2)

Case	Texture location	No of textures	Speed (RPM)	(P)max
Partially textured surface (Zone 1)	0°-180°	16	1500	1.679 MPa
			3000	3.3591 MPa
Fully textured surface (Zone 2)	0°-360°	32	1500	1.649867 MPa
			3000	3.2792 MPa

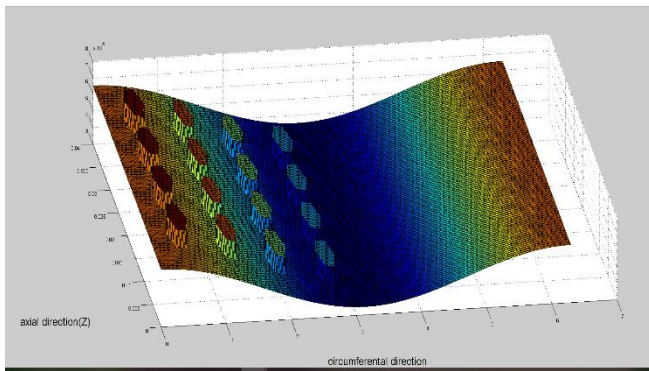


Figure 3. Film thickness profile for partially textured (zone-1) zone

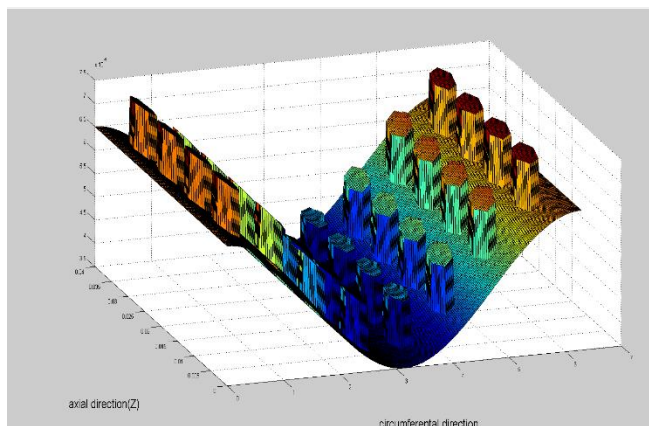
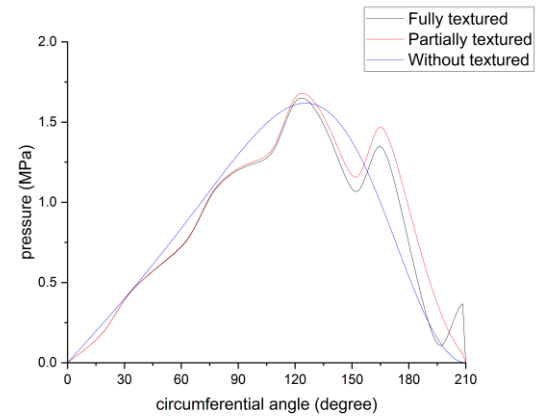
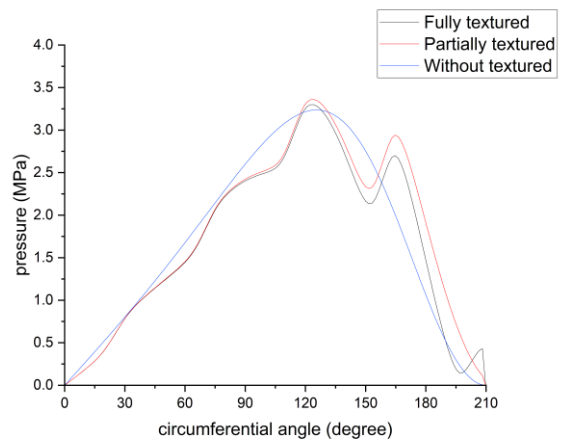


Figure 4. Film thickness profile for full textured (zone-2) zone



(a)



(b)

Figure 5: Variation of pressure in the circumferential direction for all considered surfaces (smooth, partial textured & fully textured (a) Shaft speed of 1500, (b) Shaft speed of 3000

Figures 3 and 4 depict the surface profile for film thickness in zone 1 and zone 2 respectively. It has been clearly revealed from the figures that a significant increase in film thickness is noted throughout the locations of textures. Figure 5(a) also validates the findings of previous figures where mid-plane pressures for all considered textured zones have been plotted and compared with the plain bearing case. The figure confirms that partial texture (zone 1) is showing maximum fluid film pressure in all cases. Similar trends have been obtained for higher shaft speed (3000 RPM) as shown in Figure 5(b). It has also been evident from the previous work that texture location in the maximum pressure zone i.e., convergent zone enhances the tribological properties of the journal bearing. Thus, it can be found that texturing is helpful in improving performance by taking care of its geometrical parameters.

6. CONCLUSION

The influence of hexagonal textures at textured zone 1 and zone 2 (0°-180° and 0°-360°) has been investigated. The Reynolds equation has been solved by using the central

differencing scheme of the finite difference method. The following conclusions have been observed as follows:

- Partial texturing plays a crucial role in improving the bearing performance.
- The fluid film pressure calculated for partially textured journal bearing is maximum among all cases.
- A notified difference between pressure values of partially textured bearing and plain journal bearing is observed.
- High shaft speeds and eccentricity ratio values indicate the high values of tribological properties of journal bearing.

7. ACKNOWLEDGEMENTS

This study received no funding grants from funding organizations.

REFERENCES

- [1] M. Qiu, A. Delic, and B. Raeymaekers, "The effect of texture shape on the load-carrying capacity of gas-lubricated parallel slider bearings," *Tribol Lett*, vol. 48, no. 3, pp. 315–327, Dec. 2012, doi: 10.1007/s11249-012-0027-4.
- [2] N. Sharma, S. Kango, and R. K. Sharma, "Adiabatic analysis of microtextured porous journal bearings functioned with power law fluid model," *Proceedings of the Institution of Mechanical Engineers, Part J: Journal of Engineering Tribology*, vol. 233, no. 10, pp. 1541–1553, 2019, doi: 10.1177/1350650119866026.
- [3] N. Sharma, R. Verma, S. Sharma, and S. Kango, "Qualitative potentials of surface textures and coatings in the performance of fluid-film bearings: A critical review," *Surf Topogr*, vol. 9, no. 1, p. 13002, 2021, doi: 10.1088/2051-672X/abdda0.
- [4] N. Sharma, S. Kango, R. K. Sharma, and Sunil, "Investigations on the effects of surface texture on the performance of a porous journal bearing operating with couple stress fluids," *International Journal of Surface Science and Engineering*, vol. 8, no. 4, pp. 392–407, 2014, doi: 10.1504/IJSURFSE.2014.065817.
- [5] S. Kango, N. Sharma, R. K. Sharma, and R. K. Pandey, "Experimental Investigations on Temperature and Frictional Behaviors of Textured Journal Bearings," *Tribology in Industry*, vol. 44, no. 3, pp. 508–517, Sep. 2022, doi: 10.24874/ti.1278.03.22.07.
- [6] C. B. Khatri and S. C. Sharma, "Influence of textured surface on the performance of non-recessed hybrid journal bearing operating with non-Newtonian lubricant," *Tribol Int*, vol. 95, pp. 221–235, Mar. 2016, doi: 10.1016/j.triboint.2015.11.017.
- [7] T. Nanbu, N. Ren, Y. Yasuda, D. Zhu, and Q. J. Wang, "Micro-textures in concentrated conformal-contact lubrication: Effects of texture bottom shape and surface relative motion," *Tribol Lett*, vol. 29, no. 3, pp. 241–252, Mar. 2008, doi: 10.1007/s11249-008-9302-9.
- [8] P. Maspeyrot, S. Profile, A. Bounif, N. Tala-Ighil, M. Fillon, and A. Bounif, "Hydrodynamic effects of texture geometries on journal bearing surfaces THE ANNALS OF UNIVERSITY 'DUNĂREA DE JOS' OF GALAȚI FASCICLE VIII HYDRODYNAMIC EFFECTS OF TEXTURE GEOMETRIES ON JOURNAL BEARING SURFACES," 2008. [Online]. Available: <https://www.researchgate.net/publication/258516340>
- [9] N. Sharma, S. Kango, A. Tayal, R. K. Sharma, and R. K. Sunil, "Investigations on the Influence of Surface Texturing on a Couple Stress Fluid-Based Journal Bearing by Using JFO Boundary Conditions," *Tribology Transactions*, vol. 59, no. 3, pp. 579–584, 2016, doi: 10.1080/10402004.2015.1094840.
- [10] S. Kango, R. K. Sharma, and R. K. Pandey, "Thermal analysis of microtextured journal bearing using non-Newtonian rheology of lubricant and JFO boundary conditions," *Tribol Int*, vol. 69, pp. 19–29, Jan. 2014, doi: 10.1016/J.TRIBOINT.2013.08.009.